Featured in Physics

Quantum-Path-Resolved Attosecond High-Harmonic Spectroscopy

Antoine Camper,[1,2,*] Amélie Ferré,[3] Valérie Blanchet,[4] Dominique Descamps,[4] Nan Lin,[1,5] Stéphane Petit,[4] Robert Lucchese,[6] Pascal Salières,[1] Thierry Ruchon,[1] and Yann Mairesse[4]

[1]*Université Paris-Saclay, CEA, CNRS, LIDYL, 91191 Gif-sur-Yvette, France*
[2]*Department of Physics, University of Oslo, Sem Sælandsvei 24, 0371 Oslo, Norway*
[3]*Aix Marseille Université, CNRS, LP3, 13288, Marseille, France*
[4]*Université de Bordeaux—CNRS—CEA, CELIA, UMR5107 Talence, France*
[5]*Shanghai Institute of Optics and Fine Mechanics, Chinese Academy of Sciences, 201800 Shanghai, China*
[6]*Lawrence Berkeley National Laboratory, Berkeley, California 94720, USA*

(Received 6 April 2022; accepted 8 December 2022; published 21 February 2023)

Strong-field ionization of molecules releases electrons which can be accelerated and driven back to recombine with their parent ion, emitting high-order harmonics. This ionization also initiates attosecond electronic and vibrational dynamics in the ion, evolving during the electron travel in the continuum. Revealing this subcycle dynamics from the emitted radiation usually requires advanced theoretical modeling. We show that this can be avoided by resolving the emission from two families of electronic quantum paths in the generation process. The corresponding electrons have the same kinetic energy, and thus the same structural sensitivity, but differ by the travel time between ionization and recombination—the pump-probe delay in this attosecond self-probing scheme. We measure the harmonic amplitude and phase in aligned CO_2 and N_2 molecules and observe a strong influence of laser-induced dynamics on two characteristic spectroscopic features: a shape resonance and multichannel interference. This quantum-path-resolved spectroscopy thus opens wide prospects for the investigation of ultrafast ionic dynamics, such as charge migration.

DOI: 10.1103/PhysRevLett.130.083201

Tracking charge migration in molecules is one of the main objectives of attosecond spectroscopy [1,2]. To reach this goal, two directions are being pursued. In the *ex situ* scheme, attosecond extreme ultraviolet (XUV) pulses are produced by high-order harmonic generation in a rare gas [3], and used to trigger or probe ultrafast dynamics in the medium of interest [4,5]. The *in situ* approach, also known as high-order harmonic spectroscopy (HHS), consists in using the high-order harmonic generation (HHG) process to probe the emitting medium, through a three step mechanism [6–9]. First, the strong laser field lowers the potential barrier of the target, enabling electrons to tunnel out from the highest occupied orbitals. Second, the freed electronic wave packet is accelerated by the laser field and driven back to the parent ion. Last, the electrons radiatively recombine to the ground state, emitting a burst of XUV radiation. The recombination can be seen as an interference process between the bound and accelerated parts of the wave function [10,11]. It is thus sensitive to the bound wave function's structure, encoding information into the spectrum [11,12], the phase [13,14], and the polarization state [15,16] of the emitted XUV radiation.

In this simple picture of HHS, the molecular ion is frozen between ionization and recombination. However, strong field ionization generally triggers ultrafast dynamics, leading to an attosecond evolution of the ionic core. The three-step mechanism then becomes a pump-probe scheme, in which the dynamics is initiated by tunnel ionization and probed by the recolliding electronic wave packet [17]. This configuration was first implemented to reveal the vibrational dynamics occurring in molecular ions [18,19], before being used to track the free evolution of the hole resulting from the ionization of multiple orbitals [20,21], and to reveal the existence of laser-induced hole dynamics in N_2 [22], iodoacetylene [23] or chiral molecules [24]. Several theoretical works have recently investigated the importance of subcycle multielectron dynamics in HHS, including correlation during tunneling [25] and just before recombination [26] as well as dynamical exchange [27].

In this scheme, the pump-probe delay corresponds to the time spent by the electron in the continuum. The first technique developed to map the dynamical processes relies on the natural spread of the electron trajectories in the continuum [19]—the electron travel time varies quasilinearly with the harmonic order for the short quantum paths detected in the experiments [28]. In this approach, the de Broglie wavelength of the recolliding electron varies together with the pump-probe delay, such that different spectral components of the recombination dipole moment are probed at different times. It can thus be difficult to

differentiate between structural [29] and dynamical effects [20], both being sensitive to the de Broglie wavelength but only the latter to the recombination timing. Two strategies have been used to circumvent this issue: varying the laser intensity [20,30] or the laser wavelength [23]. Both operations enable changing the electron travel time in the continuum, and thus the pump-probe delay, at a fixed de Broglie wavelength.

While they are suitable to reveal field-free dynamics [20,21], these approaches are problematic when the dynamics is driven by the strong laser field: changing the laser wavelength or intensity modifies the ionic dynamics. In practice, the evolution of the system is thus retrieved by comparing the experimental signal to theoretical calculations [22,23,31]. The complete characterization of the harmonic radiation—amplitude and phase, resolved as a function of energy and molecular alignment angle [32], as well as along the different polarization components of the emission [33–35]—provides a wealth of comparison points between experiment and theory, but does not permit the direct observation of the dynamics. This would require changing the pump-probe delay in the experiment, while keeping fixed the laser intensity and wavelength, as well as the de Broglie wavelength of the electron. In this Letter, we show that this can be achieved by making use of a well-known property of HHG: each harmonic is emitted by two electron quantum paths (QPs) labeled short and long, that have spent very different travel times in the continuum [9,36] and thus probe the target with the same de Broglie wavelength, at the same driving laser intensity, but at different delays [37]. The contributions from these two QPs can be distinguished in spatially resolved harmonic spectra [38,39]. We perform HHG in strongly aligned N_2 and CO_2 molecules using a 800 nm field, and resolve the amplitude and phase of the short and long QPs as a function of molecular alignment. HHG from these molecules are known to present distinctive features—a shape resonance in N_2 [40,41] and destructive interference between multiple channels in CO_2 [20]. We find that both effects are reflected very differently in short and long QPs, unambiguously and directly demonstrating the strong influence of the underlying attosecond dynamics on HHG.

The experiment was carried out using two laser beams generated by a phase mask [42], which, at the focus of a lens ($f = 50$ cm focal length), produces two phase-locked high-harmonic sources in a pulsed Even-Lavie supersonic gas jet [43]. A pump laser pulse prealigns the molecules in one of the two sources, inducing a change of the harmonic intensity and phase reflected in the far-field interference pattern. The spatially resolved spectrum presented in Fig. 1(a) shows harmonics from H13 to H29 produced in N_2. Each of them exhibits a well-collimated, spectrally narrow component, surrounded by a more divergent and spectrally broader ring. The spatial profile of both components is modulated by a well-contrasted interference pattern.

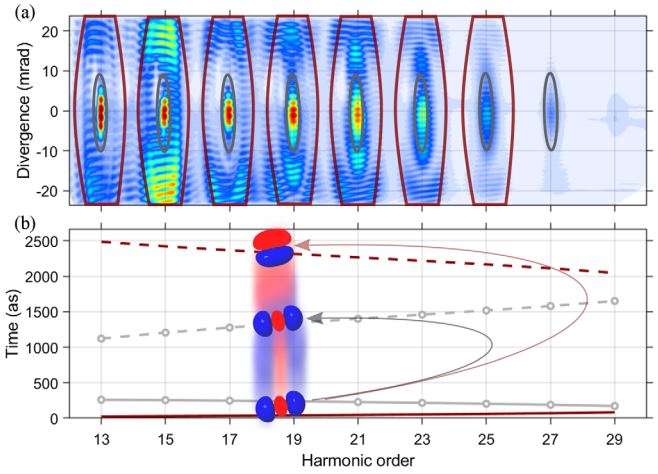

FIG. 1. (a) Spatially resolved harmonic spectrum produced by two sources in N_2 at $\sim 1.5 \times 10^{14}$ W cm^{-2}. One XUV source is generated in unaligned N_2 while the other is produced from N_2 molecules aligned at 54° from the probe polarization. The gray and red lines mark out the short and long QP contributions. (b) Calculated ionization (solid) and recombination (dashed) times for short (gray, circles) and long (red) QPs within the strong field approximation. The schematic drawing illustrates the resolution of attosecond dynamics by different QPs. An electron tunnels out from an orbital, triggering ultrafast hole dynamics in the ion. The ion has not evolved much during the short travel time of the short QP and the electron recombines to the same orbital. For the long QP, the ionic state has changed and the electron recombines to a different orbital.

The two spatiospectral components of each harmonic originate from short and long electron QPs in the HHG process. Their ionization and recombination times, calculated within the strong-field approximation (SFA) [9,44], are shown in Fig. 1(b). For H13, the travel time of the electron in the continuum is 900 as for short QPs and 2450 as for long QPs. The short and long QPs can be separated in the spectrospatial domain, as observed in Fig. 1(a) [38,45,46]. The short QPs are spatially and spectrally narrow, while the long QPs show broader divergence and spectral widths.

To extract the amplitude and phase evolution of each component of the HHG signal, we filter the contribution of short and long QPs by using the masks depicted in Fig. 1(a), and perform a Fourier analysis of the spectrally integrated spatial fringe pattern. Figures 2(a)–2(d) show the resulting evolution of the harmonic intensity and phase as a function of molecular alignment angle, for the short and long QPs. The intensities are normalized to their value at 90° and the phases are set to zero at this alignment angle. The data are symmetrized relative to the parallel alignment (0°). Note that measuring the complete phase evolution as a function of harmonic order and alignment angle would require the use of photoelectron spectroscopy [32], which prevents the resolution of short and long trajectories. Alternatively, more complex interferometric schemes with

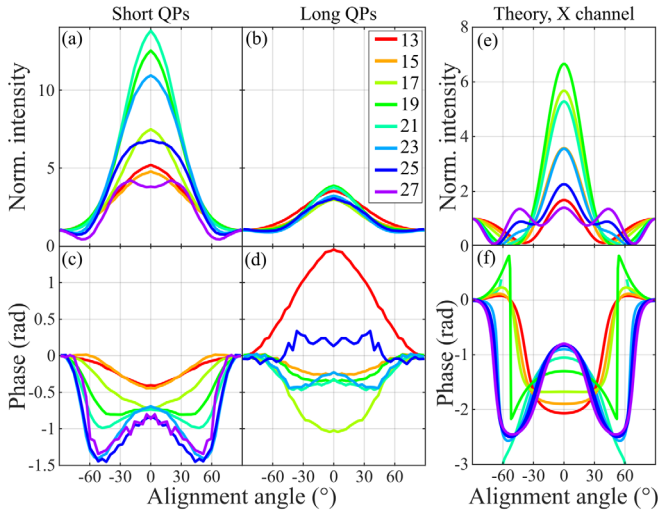

FIG. 2. Intensity (a), (b) and phase (c), (d) of the short (a), (c) and long (b), (d) QP contributions to high-harmonic generation in aligned N_2. (e) Calculated modulus square and (f) phase of the molecular-frame scattering-wave recombination dipole matrix element to the X channel.

an atomic reference could enable resolving the complete phase evolution of the harmonic emission [47].

For short QPs, the modulation of the harmonic emission with molecular alignment shows a very high contrast around H19–23. For instance, the signal from H21 is 14 times stronger when the molecules are parallel to the driving laser polarization than when they are perpendicular. As the harmonic order further increases, the modulation contrast decreases, and the harmonic emission shows local minima around 60° and a local maximum around 0°, except for H27 which presents a local minimum at 0°. The phase measurement reveals an interesting evolution as well. The curvature of the phase variation around 0° reverses when the harmonic order increases, from positive for H13–17 to negative above H19. A phase jump around 60° also gradually appears, maximizing to around 1.5 rad in the cutoff (H23–27).

Turning to the long QPs, we observe a dramatically different behavior. All harmonics show a very similar intensity modulation contrast, around 3. The highest harmonics present a local minimum at 60°. The phase of H13 shows an evolution opposite to all other harmonics (as well as short QPs), with a large 1.5 rad excursion. This strong difference between short and long QPs for this harmonic is consistent with the recent measurements of [48], who observed a π shift in the relative phase of short and long QPs between 0° and 90° for the integrated harmonic emission between H11 and H15. For H15, we find that the phase evolution is remarkably similar to the one of the short QP, and for H17 the phase modulation is more contrasted in the long QP. Harmonics 19–23 only show weak variations. The contributions from short and long QPs merge above H25 due to the proximity of the harmonic cutoff (see Fig. 1). We thus only present H27 on the short QPs plot.

The harmonic emission from the short and long QPs show drastically different amplitude and phase evolutions as a function of molecular alignment angle. The strong intensity modulation of the short QPs around H19–23 (29.5–35.7 eV) is the signature of a shape resonance in the photorecombination cross section of the X channel (associated with the highest occupied molecular orbital HOMO) [41], as shown in the theoretical molecular-frame scattering-wave recombination dipole matrix element [Fig. 2(e)] [49,50]. The calculated phase of the photorecombination dipole moment in the X channel [Fig. 2(f)] shows a remarkable qualitative agreement with the measured phase evolution of the short QPs, with a reversal of curvature at 0° around H19 and sudden phase jumps around 60° for high orders. Theoretical studies have shown that if the ion remains steady between ionization and recombination, shape resonances affect short and long QPs in a similar manner [32,51]. Our results show the opposite and thus demonstrate the existence of a subcycle dynamics in the ion. The shape resonance appears when electrons are trapped by the potential barrier in the X channel before recombining. If the laser excites the ion between ionization and recombination, the electrons can recombine to deeper orbitals, e.g., to the HOMO-1 (associated with the A channel) [22]. These cross-channels are not sensitive to the shape resonance, which is a single-electron effect with no interchannel couplings [52]. Long QPs, probing the system at longer times than short QPs, reveal the higher proportion of excited ionic states characterized by intensity and phase variations that are very different from that dictated by the shape resonance in the X channel.

As a second illustration of the interest of QP-resolved HHS, we analyze the results of measurements in CO_2 at 0.8×10^{14} W cm^{-2}, in which characteristic destructive interference between contributions from the HOMO (X channel) and HOMO-2 (B channel) is known to occur when molecules are aligned around 0° [20]. Figures 3(a) and 3(b) show the harmonic intensity as a function of the alignment angle, for short and long QPs. For short QPs, the destructive interference appears as a local minimum of the intensity around 25° at H19, and shifts to higher angles as the harmonic order increases [Fig. 3(a)]. It is associated with a jump of the harmonic phase as a function of molecular alignment, reaching 2.3 rad around 30° for H23 [Fig. 3(c)]. The signal from long QPs is quite different, showing no such sign of interference minimum and phase jump.

If the ionic populations do not evolve between ionization and recombination, then the relative phase between interfering channels is $\Delta\varphi^{XB} \simeq \Delta\varphi_0^{XB} + (Ip^B - Ip^X)\tau + \Delta\varphi_{\mathrm{rec}}^{XB}$, where $\Delta\varphi_0^{XB}$ is the initial relative phase between the ionic states populated by tunnel ionization, τ is the electron travel time in the continuum, Ip^j is the ionization potential of channel j and $\Delta\varphi_{\mathrm{rec}}^{XB}$ the phase difference between the recombination dipole moments of the two channels, which

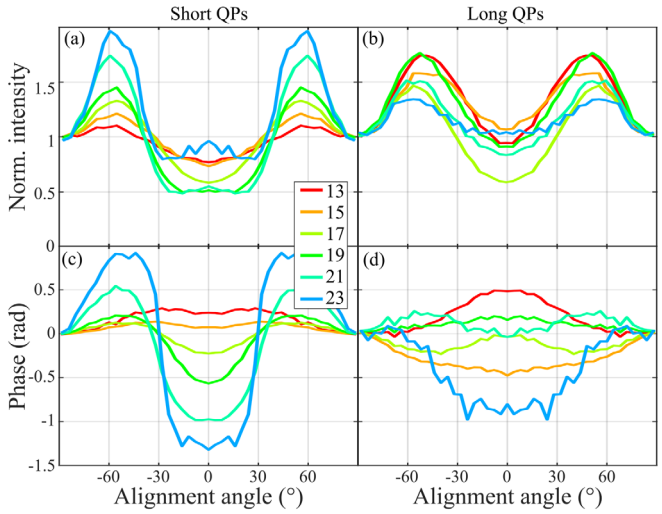

FIG. 3. Quantum-path-resolved high-harmonic spectroscopy in CO_2. Amplitude for short (a) and long (b) QPs and phase evolution for short (c) and long (d) QPs.

is $\sim 0.5\pi$ around H21–27 [20]. The dynamical interference minimum in HHG from CO_2 occurs when $\Delta\varphi^{XB} = (2n + 1)\pi$ with $n \in \mathbb{Z}$. Previous work on short QP established that $\Delta\varphi_0^{XB} = 0$ [20]. The condition for destructive interference is then fulfilled for electron travel times $\tau \approx 1.2$ fs. This is consistent with our measurement of a minimum at H19 and a phase jump on the short QPs. Destructive interference is also expected when $\tau \approx 2.15$ fs, which is the travel time of long QPs around H19–21. Thus, in the absence of additional ionic dynamics, the destructive interference between channels X and B is expected to occur at the same harmonic order for short and long QPs. This is clearly not the case in our measurements—the long QPs show no destructive interference minimum, and no large phase jump [Figs. 3(b) and 3(d)]. This demonstrates the influence of the dynamical evolution of the ion in the time window between 1 and 2 fs after ionization. This is consistent with the recent calculations of Shu *et al.*, who demonstrated the importance of a laser-induced coupling between the B and C states of CO_2 molecules aligned parallel to a 800 nm laser field [53]. This coupling enables electrons tunneling from the HOMO-2 to recombine to the HOMO-3, opening a new cross channel in the process. Interestingly, Shu *et al.* found that for short QPs, these dynamics hardly affect the interference minimum between X and B channels. This explains why they had remained unaccounted for until now. In contrast, in the case of long QPs the system has enough time to evolve between ionization and recombination. These QPs thus carry information relative to the HOMO-2/HOMO-3 cross channel. This stresses the importance of QP-resolved high-harmonic spectroscopy to track such attosecond dynamics.

In conclusion, using two prototypical cases, we have demonstrated the ability of quantum-path-resolved high-harmonic spectroscopy to reveal the attosecond dynamics between ionization and recombination. In CO_2, the destructive interference and phase jump between X and B channels observed in the short QPs disappears at long electron excursion times, reflecting the coupling between B and C channels [53]. In N_2, the influence of the shape resonance in the X channel, which strongly affects the short QPs response, disappears at long excursion times, suggesting a recombination to a deeper, nonresonant channel. Both features illustrate the important role of laser-induced couplings in high-harmonic spectroscopy. These couplings, predicted by theory [22,53], are often neglected because they are difficult to disentangle from structural effects in conventional high-harmonic spectroscopy experiments, but clearly appear in QP-resolved measurements. Such investigations could also be extended to condensed matter, where short and long QPs have recently been identified [54], to unravel attosecond hole dynamics in semiconductors.

We thank R. Bouillaud, N. Fedorov, and L. Merzeau for technical assistance. This project has received funding from the European Research Council (ERC) under the European Union's Horizon 2020 research and innovation program No. 682978—EXCITERS, from Agence Nationale de la Recherche (ANR-14-CE32-0010–Xstase), and from the Research Council of Norway under Grant Agreement No. 303337. Work at LBNL supported by U.S. Department of Energy, Office of Science, Basic Energy Sciences, Chemical Sciences, Geosciences, Biosciences Division (DE-AC02-05CH11231).

The authors declare no conflict of interest.

*Corresponding author.
antoine.camper@fys.uio.no

[1] F. Remacle and R. D. Levine, Proc. Natl. Acad. Sci. U.S.A. **103**, 6793 (2006).
[2] F. Lépine, M. Y. Ivanov, and M. J. J. Vrakking, Nat. Photonics **8**, 195 (2014).
[3] M. Chini, K. Zhao, and Z. Chang, Nat. Photonics **8**, 178 (2014).
[4] F. Calegari, D. Ayuso, A. Trabattoni, L. Belshaw, S. D. Camillis, S. Anumula, F. Frassetto, L. Poletto, A. Palacios, P. Decleva, J. B. Greenwood, F. Martín, and M. Nisoli, Science **346**, 336 (2014).
[5] T. Okino, Y. Furukawa, Y. Nabekawa, S. Miyabe, A. A. Eilanlou, E. J. Takahashi, K. Yamanouchi, and K. Midorikawa, Sci. Adv. **1**, e1500356 (2015).
[6] M. Y. Kuchiev, Pis'ma Zh. Eksp. Teor. Fiz. **45**, 319 (1987).
[7] J. L. Krause, K. J. Schafer, and K. C. Kulander, Phys. Rev. Lett. **68**, 3535 (1992).
[8] P. B. Corkum, Phys. Rev. Lett. **71**, 1994 (1993).
[9] M. Lewenstein, P. Balcou, M. Y. Ivanov, A. L'Huillier, and P. B. Corkum, Phys. Rev. A **49**, 2117 (1994).
[10] A. Pukhov, S. Gordienko, and T. Baeva, Phys. Rev. Lett. **91**, 173002 (2003).
[11] J. Itatani, J. Levesque, D. Zeidler, H. Niikura, H. Pepin, J. C. Kieffer, P. B. Corkum, and D. M. Villeneuve, Nature (London) **432**, 867 (2004).

[12] C.-G. Wahlström, J. Larsson, A. Persson, T. Starczewski, S. Svanberg, P. Salières, P. Balcou, and A. L'Huillier, Phys. Rev. A **48**, 4709 (1993).

[13] W. Boutu, S. Haessler, H. Merdji, P. Breger, G. Waters, M. Stankiewicz, L. J. Frasinski, R. Taieb, J. Caillat, A. Maquet, P. Monchicourt, B. Carre, and P. Salieres, Nat. Phys. **4**, 545 (2008).

[14] X. Zhou, R. Lock, W. Li, N. Wagner, M. M. Murnane, and H. C. Kapteyn, Phys. Rev. Lett. **100**, 073902 (2008).

[15] J. Levesque, Y. Mairesse, N. Dudovich, H. Pépin, J.-C. Kieffer, P. B. Corkum, and D. M. Villeneuve, Phys. Rev. Lett. **99**, 243001 (2007).

[16] X. Zhou, R. Lock, N. Wagner, W. Li, H. C. Kapteyn, and M. M. Murnane, Phys. Rev. Lett. **102**, 073902 (2009).

[17] C. D. Lin, A.-T. Le, Z. Chen, T. Morishita, and R. Lucchese, J. Phys. B **43**, 122001 (2010).

[18] M. Lein, Phys. Rev. Lett. **94**, 053004 (2005).

[19] S. Baker, Science **312**, 424 (2006).

[20] O. Smirnova, Y. Mairesse, S. Patchkovskii, N. Dudovich, D. Villeneuve, P. Corkum, and M. Y. Ivanov, Nature (London) **460**, 972 (2009).

[21] S. Haessler, J. Caillat, W. Boutu, C. Giovanetti-Teixeira, T. Ruchon, T. Auguste, Z. Diveki, P. Breger, A. Maquet, B. Carré, R. Taïeb, and P. Salières, Nat. Phys. **6**, 200 (2010).

[22] Y. Mairesse, J. Higuet, N. Dudovich, D. Shafir, B. Fabre, E. Mével, E. Constant, S. Patchkovskii, Z. Walters, M. Y. Ivanov, and O. Smirnova, Phys. Rev. Lett. **104**, 213601 (2010).

[23] P. M. Kraus, B. Mignolet, D. Baykusheva, A. Rupenyan, L. Horný, E. F. Penka, G. Grassi, O. I. Tolstikhin, J. Schneider, F. Jensen, L. B. Madsen, A. D. Bandrauk, F. Remacle, and H. J. Wörner, Science **350**, 790 (2015).

[24] R. Cireasa, A. E. Boguslavskiy, B. Pons, M. C. H. Wong, D. Descamps, S. Petit, H. Ruf, N. Thiré, A. Ferré, J. Suarez, J. Higuet, B. E. Schmidt, A. F. Alharbi, F. Légaré, V. Blanchet, B. Fabre, S. Patchkovskii, O. Smirnova, Y. Mairesse, and V. R. Bhardwaj, Nat. Phys. **11**, 654 (2015).

[25] L. Torlina, M. Ivanov, Z. B. Walters, and O. Smirnova, Phys. Rev. A **86**, 043409 (2012).

[26] M. Ruberti, P. Decleva, and V. Averbukh, Phys. Chem. Chem. Phys. **20**, 8311 (2018).

[27] V. P. Majety and A. Scrinzi, Phys. Rev. Lett. **115**, 103002 (2015).

[28] Y. Mairesse, A. de Bohan, L. J. Frasinski, H. Merdji, L. C. Dinu, P. Monchicourt, P. Breger, M. Kovacev, R. Taïeb, B. Carré, H. G. Muller, P. Agostini, and P. Salières, Science **302**, 1540 (2003).

[29] M. Lein, N. Hay, R. Velotta, J. P. Marangos, and P. L. Knight, Phys. Rev. A **66**, 023805 (2002).

[30] D. R. Austin, A. S. Johnson, F. McGrath, D. Wood, L. Miseikis, T. Siegel, P. Hawkins, A. Harvey, Z. Mašín, S. Patchkovskii, M. Vacher, J. P. Malhado, M. Y. Ivanov, O. Smirnova, and J. P. Marangos, Sci. Rep. **11**, 2485 (2021).

[31] B. D. Bruner, D. Azoury, G. Orenstein, H. R. Larsson, M. Krüger, N. Dudovich, and S. Bauch, Nat. Commun. **8**, 1453 (2017).

[32] A. Camper, E. Skantzakis, R. Géneaux, F. Risoud, E. English, E. English, Z. Diveki, N. Lin, V. Gruson, T. Auguste, B. Carré, R. R. Lucchese, A. Maquet, R. Taïeb, J. Caillat, T. Ruchon, and P. Salières, Optica **8**, 308 (2021).

[33] A. Camper, A. Ferré, V. Blanchet, F. Burgy, D. Descamps, S. Petit, T. Ruchon, and Y. Mairesse, Opt. Lett. **40**, 5387 (2015).

[34] A. Ferré, H. Soifer, O. Pedatzur, C. Bourassin-Bouchet, B. D. Bruner, R. Canonge, F. Catoire, D. Descamps, B. Fabre, E. Mével, S. Petit, N. Dudovich, and Y. Mairesse, Phys. Rev. Lett. **116**, 053002 (2016).

[35] A. J. Uzan, H. Soifer, O. Pedatzur, A. Clergerie, S. Larroque, B. D. Bruner, B. Pons, M. Ivanov, O. Smirnova, and N. Dudovich, Nat. Photonics **14**, 188 (2020).

[36] M. B. Gaarde, Opt. Express **8**, 529 (2001).

[37] A. Zaïr, T. Siegel, S. Sukiasyan, F. Risoud, L. Brugnera, C. Hutchison, Z. Diveki, T. Auguste, J. W. Tisch, P. Salières, M. Y. Ivanov, and J. P. Marangos, Chem. Phys. **414**, 184 (2013).

[38] M. Bellini, C. Lyngå, A. Tozzi, M. B. Gaarde, T. W. Hänsch, A. L'Huillier, and C. G. Wahlström, Phys. Rev. Lett. **81**, 297 (1998).

[39] F. Catoire, A. Ferré, O. Hort, A. Dubrouil, L. Quintard, D. Descamps, S. Petit, F. Burgy, E. Mével, Y. Mairesse, and E. Constant, Phys. Rev. A **94**, 063401 (2016).

[40] C. Jin and C. D. Lin, Phys. Rev. A **85**, 033423 (2012).

[41] X. Ren, V. Makhija, A.-T. Le, J. Troß, S. Mondal, C. Jin, V. Kumarappan, and C. Trallero-Herrero, Phys. Rev. A **88**, 043421 (2013).

[42] A. Camper, A. Ferré, N. Lin, E. Skantzakis, D. Staedter, E. English, B. Manschwetus, F. Burgy, S. Petit, D. Descamps, T. Auguste, O. Gobert, B. Carré, P. Salières, Y. Mairesse, and T. Ruchon, Photonics **2**, 184 (2015).

[43] U. Even, J. Jortner, D. Noy, N. Lavie, and C. Cossart-Magos, J. Chem. Phys. **112**, 8068 (2000).

[44] P. Salières, B. Carré, L. Le Déroff, F. Grasbon, G. Paulus, H. Walther, R. Kopold, W. Becker, D. Milošević, A. Sanpera, and others, Science **292**, 902 (2001).

[45] P. Salières, A. L'Huillier, and M. Lewenstein, Phys. Rev. Lett. **74**, 3776 (1995).

[46] F. Catoire, A. Ferré, O. Hort, A. Dubrouil, L. Quintard, D. Descamps, S. Petit, F. Burgy, E. Mével, Y. Mairesse, and E. Constant, Phys. Rev. A **94**, 063401 (2016).

[47] D. Azoury, O. Kneller, S. Rozen, B. D. Bruner, A. Clergerie, Y. Mairesse, B. Fabre, B. Pons, N. Dudovich, and M. Krüger, Nat. Photonics **13**, 54 (2018).

[48] S. Chatziathanasiou, I. Liontos, E. Skantzakis, S. Kahaly, M. U. Kahaly, N. Tsatrafyllis, O. Faucher, B. Witzel, N. Papadakis, D. Charalambidis, and P. Tzallas, Phys. Rev. A **100**, 061404(R) (2019).

[49] R. R. Lucchese, G. Raseev, and V. McKoy, Phys. Rev. A **25**, 2572 (1982).

[50] R. E. Stratmann, G. Bandarage, and R. R. Lucchese, Phys. Rev. A **51**, 3756 (1995).

[51] M. Tudorovskaya and M. Lein, Phys. Rev. A **84**, 013430 (2011).

[52] M. Piancastelli, J. Electron Spectrosc. Relat. Phenom. **100**, 167 (1999).

[53] Z. Shu, H. Liang, Y. Wang, S. Hu, S. Chen, H. Xu, R. Ma, D. Ding, and J. Chen, Phys. Rev. Lett. **128**, 183202 (2022).

[54] Y. W. Kim, T.-J. Shao, H. Kim, S. Han, S. Kim, M. Ciappina, X.-B. Bian, and S.-W. Kim, ACS Photonics **6**, 851 (2019).